Inorganic Chemistry

Article

pubs.acs.org/IC

In Situ Observation of Gating Phenomena in the Flexible Porous Coordination Polymer $Zn_2(BPnDC)_2(bpy)$ (SNU-9) in a Combined Diffraction and Gas Adsorption Experiment

Volodymyr Bon,[†] Irena Senkovska,[†] Dirk Wallacher,[‡] Daniel M. Többens,[§] Ivo Zizak,[∥] Ralf Feyerherm,[⊥] Uwe Mueller,[¶] and Stefan Kaskel*[,†]

[†]Department of Inorganic Chemistry, Dresden University of Technology, Bergstrasse 66, 01069, Dresden, Germany

[‡]Department Sample Environments, Helmholtz Centre Berlin for Materials and Energy, Hahn-Meitner Platz 1, 14109 Berlin, Germany

[§]Department of Crystallography, Helmholtz Centre Berlin for Materials and Energy, Albert-Einstein-Strasse 15, 12489 Berlin, Germany

[∥]Institute of Nanometer Optik and Technology, Helmholtz Centre Berlin for Materials and Energy, Albert-Einstein-Strasse 15, 12489 Berlin, Germany

[⊥]Institute of Complex Magnetic Materials, Helmholtz Centre Berlin for Materials and Energy, Albert-Einstein-Strasse 15, 12489 Berlin, Germany

[¶]Macromolecular Crystallography Group, Institute Soft Matter and Functional Materials, Albert-Einstein-Strasse 15, 12489 Berlin, Germany

Supporting Information

ABSTRACT: The intrinsic structural dynamic during the adsorption of CO_2 at 195 K and N_2 at 77 K on flexible porous coordination polymer $Zn_2(BPnDC)_2(bpy)$ (SNU-9) was studied in situ by powder XRD. The crystal structures of as made and solvent free (activated) phases were determined by single crystal X-ray diffraction. During the structural transformation caused by activation, the rearrangement of Zn−O bonds occurs that leads to changes in coordination environment of Zn atoms. Such changes lead to the contraction of the unit cell and to decreasing unit cell volume of nearly 28% in comparison to the pristine as made structure. The solvent accessible volume of the unit cell decreases from 40.8% to 12.8%. The adsorption of CO_2 and N_2 on SNU-9 proceeds in a different way: the formation of intermediate phase during the CO_2 adsorption could be postulated, while the transformation from narrow pore form to the open structure occurs in quasi-one-step in the case of N_2 adsorption (the intermediate phase is formed only in very narrow pressure region). The transformation of the structure is guest dependent and the differences in the structures of CO_2@SNU-9 at 195 K and N_2@SNU-9 at 77 K were proven by Pawley and Rietveld refinements of powder XRD patterns. The structure of N_2@SNU-9 is identical to this of as synthesized phase, while the structure of CO_2@SNU-9 differs slightly.

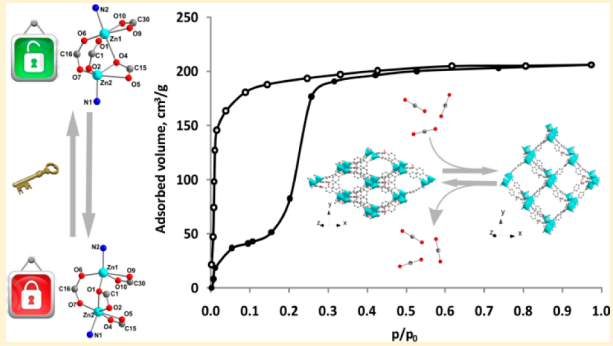

INTRODUCTION

Crystalline porous materials (PCPs or MOFs), constructed from multidentate organic ligands and metal clusters using modular building concept,[1−4] were widely studied during past decade because of their fascinating properties. Enormous surface areas and pore volumes[5,6] make them excellent candidates to be used as gas storage materials.[7−11] Tunable pores open another field of application in separation processes[12−17] and in heterogeneous catalysis.[18−21] The possibility to create open metal sites on the inner surface, as well the quite simple possibility to functionalize the organic component of the framework (before MOF synthesis or postsynthetically), allow for a wide range of surface functionalities, as well as afford the opportunity to control the framework flexibility. Since third generation of PCPs,[22] so-called "gate pressure" or "breathable" MOFs were discovered some years ago, the fascinating feature to change the crystal structure and adsorption properties as a response to well-defined external stimuli like guest molecules,[23−25] temperature, or electromagnetic irradiation[26] engages the researchers of different field of science. More and more understanding of the phenomenon itself was won but also further potential application fields were recognized. For example, the amine

Received: October 1, 2013
Published: January 17, 2014

   dx.doi.org/10.1021/ic4024844 | Inorg. Chem. 2014, 53, 1513−1520

functionalized MIL-53 material (MIL = Matériaux de l'Institut Lavoisier) was found to be useful as reversible optical switch[27] and as appropriate membrane material for CO_2/CH_4 separation.[28] Cu-SIP-3 material, reported by Morris et al.[29] shows an excellent performance in selective NO adsorption. Kitagawa and co-workers have successfully incorporated the stimuli responsible linker into a PCP and obtained a material with optical switchable adsorption properties.[26]

One of the suitable methods to monitor the changes in the crystal structure during adsorption is combined adsorption and X-ray diffraction, which should facilitate not only the detection, but in the best case also the direct visualization of structural changes via structure solution and refinement.

Up to now, a plethora of flexible MOF materials was investigated in situ by X-ray diffraction;[30,31] nevertheless, the structural analysis from the collected data remain an issue. Materials with stepwise adsorption[32,33] are of special interest here due to the possible formation of intermediate structures during the adsorption, which can be detected only by in situ experiments.

In this contribution, we report on the intrinsic structural dynamics of the flexible MOF $Zn_2(BPnDC)_2(bpy)$ (BPnDC, benzophenone 4,4′-dicarboxylic acid, bpy, 4,4′-bipyridine), also known as SNU-9,[34] investigated in situ during physisorption of N_2 at 77 K and CO_2 at 194.5 K.

EXPERIMENTAL SECTION

In Situ Adsorption via X-ray Powder Diffraction Experiments. Concerted adsorption and X-ray powder diffraction experiments were performed at Helmholtz-Zentrum Berlin für Materialien and Energie on KMC-2 beamline. The detailed description of the measuring set up is provided in ref 35. The X-ray with wavelength of 1.5406 Å, a 0.2 × 0.2 mm beam and a 2D General Area Detector Diffraction System (GADDS) VÅNTEC 2000 from Bruker, positioned with 620 mm distance from the sample were used for all diffraction experiments. To eliminate the reflections from the partially crystalline Be-dome, a tungsten slit aperture with 5 mm opening was mounted horizontally on the detectors nose. Collected data were integrated using Datasqueeze software. Hexagonal boron nitride was used as external standard.

To protect the sample from the ambient humidity, all sample preparation steps were performed in argon atmosphere (Glove Box). The powdered sample with crystallite grains ≤45 μm was loaded between two Kapton films providing the thickness of the sample nearly 1 mm.

The sample chamber is tightly closed with a small Be-dome, making the system transparent for X-rays. The sample chamber is connected with automated dosing system BELSORP-max using a copper capillary and Swagelok fittings. The gas dosing system is connected with goniometer control computer by electronic dongle that transmit impulses in both directions.

The X-ray diffraction patterns were measured in transmission geometry with 2θ scans with 2° steps from 5° to 70° 2θ. The sample was kept at a constant tilt angle of 30°. The adsorption measurements were performed with N_2 and CO_2 as adsorptive at 77.3 and 194.5 K, respectively. Pawley refinement of the activated and N_2@SNU-9 phases was performed using Reflex tool of Material Studio 5.0.[36] The same tool was used for indexing, Pawley and Rietveld refinements combined with force field energy minimization of CO_2@SNU-9 phase.

The crystal structure of as made phase was used as starting model for the Rietveld refinement, in combination with the unit cell parameters, obtained from the indexing and Pawley refinement of CO_2@SNU-9 PXRD pattern. Accordingly to the physisorption isotherm, 84 molecules of CO_2 per unit cell are adsorbed at p/p_0 = 0.974. Because the number of formula units in the cell is eight, 80 CO_2 molecules were introduced into the framework voids for Rietveld refinement. The results of rigid body Rietveld refinement are given in Supporting Information (Figures S10 and S11). CCDC-974276 contains the supplementary crystallographic data for CO_2@SNU-9 compound. These data can be obtained free of charge from the Cambridge Crystallographic Data Centre via www.ccdc.cam.ac.uk/data_request/cif.

Single-Crystal X-ray Diffraction Study. The investigated compound was synthesized and activated for the adsorption experiments following the published procedure.[34] The as made single crystal of SNU-9 was washed with fresh *N,N*-dimethylformamid (DMF) and placed into the glass capillary with some amount of solvent. The capillary was sealed with melted wax. The single crystal of activated SNU-9 (high vacuum overnight at 60 °C) was fixed with glue on the glass needle. The data sets were collected at beamline BL14.2, Joint Berlin-MX Laboratory of Helmholtz Zentrum Berlin für Materialien und Energie, equipped with a MX-225 CCD detector (Rayonics, Illinois) and 1-axes goniometer.[37] The monochromator was set to the energy of 14 keV (λ = 0.88561 Å). The collected data were integrated and scaled using Mosflm 1.0.5 and Scala programs, respectively.[38] The structures were solved by direct methods and refined by full-matrix least-squares on F^2 using SHELXS and SHELXL[39] programs, respectively. All non-hydrogen atoms were refined in anisotropic approximation. The hydrogen atoms were positioned geometrically and refined using a riding model. Although the lattice solvent molecules (2 DEF and 1 methanol) could not be determined from difference Fourier map because of disorder, they were included in the composition and formula weight of as made phase. The main experimental data of single crystal X-ray diffraction experiments are given in Table 1. CCDC-961805 and 961806 contain the supplementary crystallographic data.

Table 1. Crystal Data on SNU-9_as-made and SNU-9_activated

	SNU-9_as-made	SNU-9_activated
chemical formula	$C_{51}H_{50}N_4O_{13}Zn_2$	$C_{40}H_{24}N_2O_{10}Zn_2$
formula weight	1057.35	823.35
space group	*C*2/*c*	*C*2/*c*
a (Å)	21.150(4)	26.230(5)
b (Å)	18.850(4)	10.680(2)
c (Å)	26.200(5)	27.040(5)
β (deg)	102.90(3)	104.50(3)
V (Å^3)	10182(3)	7334(2)
Z	8	8
T (K)	293	293
λ (Å)	0.88561	0.88561
D_{calc} (g·cm^{-3})	1.074	1.491
μ (mm^{-1})	1.776	2.466
R ($I > 2\sigma(I)$)[a]	0.0724	0.0534
Rw (all data)[a]	0.2172	0.1369
S	1.144	1.150

[a] $R = \sum_{h,k,l}||F_O| - |F_C||/\sum_{h,k,l}|F_O|$; $Rw = [(\sum_{h,k,l}w(|F_O^2| - |F_C^2|)^2)/(\sum_{h,k,l}w|F_O^2|)]^{1/2}$.

RESULTS AND DISCUSSION

Recently, Park et al. reported a doubly interpenetrated MOF with a composition $[Zn_2(BPnDC)_2(bpy)]_2(DEF)_2(MeOH)$ (further referred to as SNU-9_as-made) (BPnDC, benzophenone 4,4′-dicarboxylic acid, bpy, 4,4′-bipyridine, DEF, *N,N*-diethylformamide). The gas adsorption isotherms of the desolvated compound $Zn_2(BPnDC)_2(bpy)$ (SNU-9_activated) show three-step adsorption for N_2 (at 77 K) and O_2 (87 K) and two-step adsorption for CO_2 (195 K) and H_2 (77 K) with large hysteresis on desorption.

The aim of this work was to investigate the structural dynamic during the adsorption of guest molecules. The crystal

dx.doi.org/10.1021/ic4024844 | Inorg. Chem. 2014, 53, 1513−1520

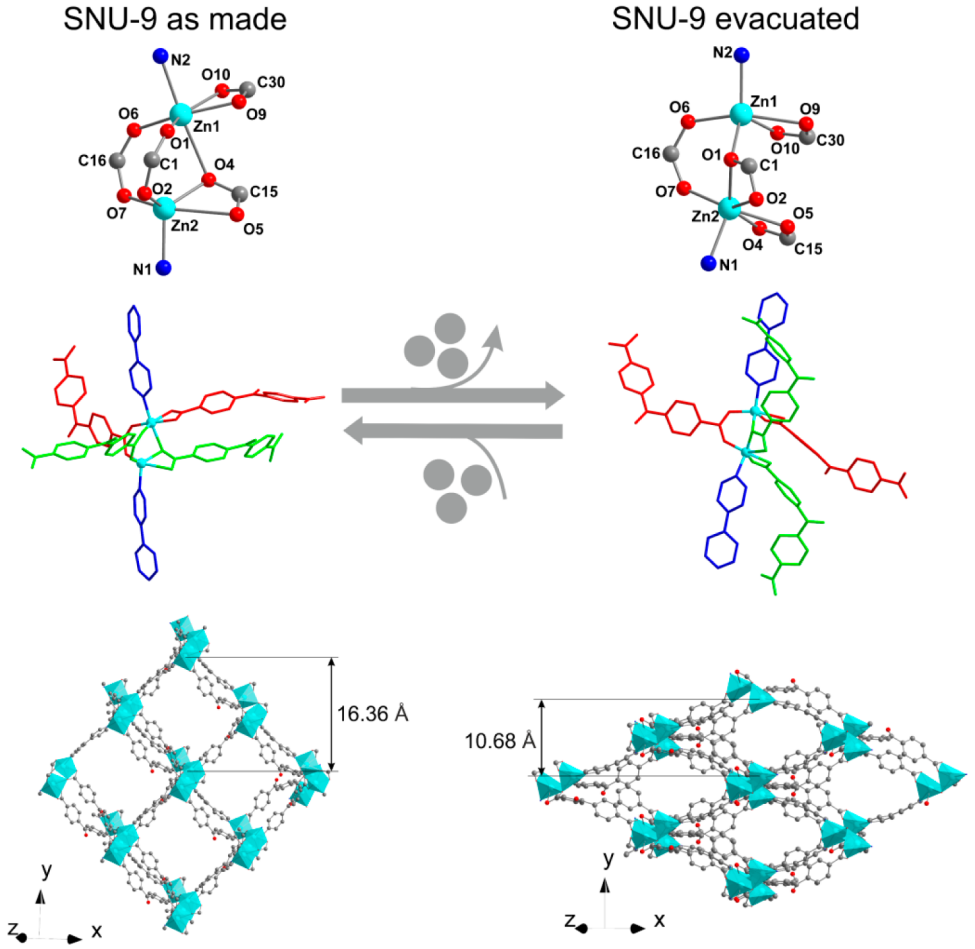

Figure 1. Crystal structure of SNU-9 as made (left) and SNU-9 evacuated (right) phases: SBU geometry (top), ligands arrangement around SBUs (middle), and view on a single framework along [101] direction (bottom).

structures of SNU-9_as-made as well as for methanol exchanged compound $[Zn_2(BPnDC)_2(bpy)](MeOH)_6$ at 100 K were reported by Park et al.[34] The unit cell parameters, reported for SNU-9_as-made differ slightly from unit cell parameters determined at 293 K (this study Table 1), however both structures are almost identical.

The structure consists of unusual asymmetric paddle-wheels SBU, composed of two Zn atoms coordinated by four carboxylic groups from BPnDC linkers and two nitrogen atoms from 4,4′-bipyridine molecules in the axial positions. Two Zn atoms and 4,4′-bipyridine molecules are not linear arranged, as it is usual for paddle-wheel pillar-layer frameworks.[40,41] Two carboxylic groups O1—C1—O2 and O6—C16—O7, belonging to the symmetry independent ligands, coordinate two zinc atoms of the cluster in bridging μ-carboxylato-κO:κO′ mode with similar Zn−O distances (2.006(3), 1.936(3), 2.017(2), and 1.968(2) Å). The remaining two carboxylic groups O4—C15—O5 and O9—C30—O10 are coordinated to Zn1 and Zn2, respectively, in chelating fashion. One of them is additionally connected to Zn1 (Zn1—O4 distance 2.474(3) Å). The coordination geometry of the zinc atoms in the cluster could be described as strongly distorted octahedral for Zn1 and distorted square-pyramidal for Zn2 (see Supporting Information for bond lengths and angles).

The distance between two Zn atoms in the cluster is 3.21 Å, which is significantly larger in comparison with "classical" paddle wheel SBU (in average 2.7 Å). Such type of cluster was observed by Bharadwaj et al. in a similar coordination polymer, in which 4-(methoxycarbonyl)benzoate and 4,4′-bipyridine were used as linkers.[42] SNU-9 contains two interpenetrated frameworks related by inversion center, adopting **pcu** topology. The shortest distance between symmetry dependent Zn atoms, which belong to different frameworks is 7.629(4) Å. The unit cell of SNU-9_as-made contains 40.8% solvent accessible void, calculated using PLATON.[43]

The SNU-9_as-made sample was soaked with methanol, and subsequently activated in high vacuum at 60 °C. The single crystal suitable for X-ray diffraction experiment was transferred to Paratone oil and mounted on a glass fiber. The crystal structure was solved in *C*2/*c* space group with quantitative identical content of asymmetric unit.

Analysis of the evolution of unit cell parameters shows significant changes in the *b* axis, which became nearly two times shorter after the activation procedure (Table 1). It is accompanied by moderate increasing of *a* axis length and monoclinic angle enhancement. Such changes in the unit cell parameters cause decreasing of unit cell volume of nearly 28% in comparison to the pristine open as made structure. The solvent accessible unit cell volume decreases from 40.8% to 12.8%.

The detailed analysis of the structure reveals significant changes in the coordination environment of Zn atoms and the cluster. The coordination geometry of Zn1 atom evolves from distorted octahedral (adjacent angles range 60.30(9)—

dx.doi.org/10.1021/ic4024844 | *Inorg. Chem.* 2014, 53, 1513−1520

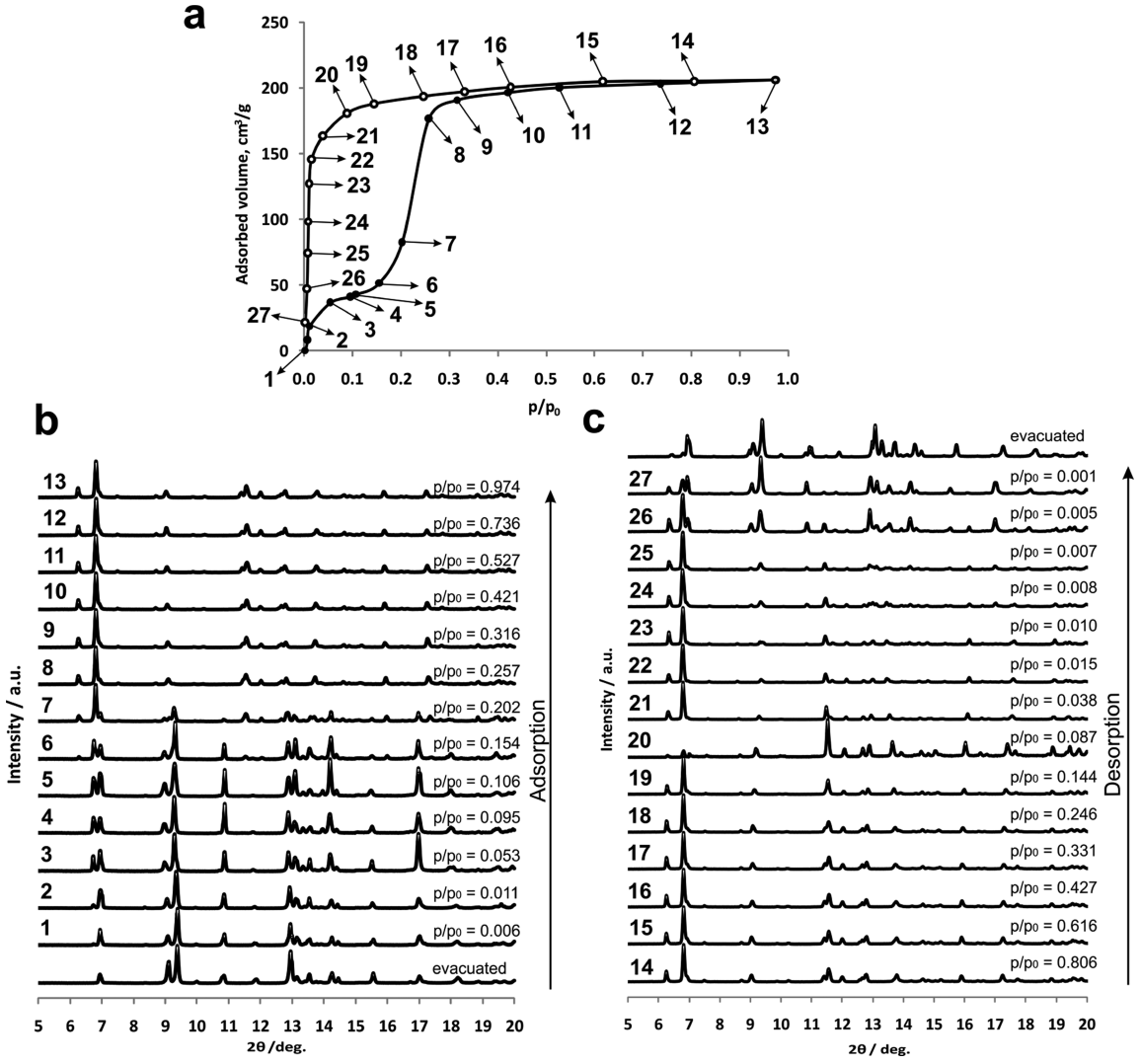

Figure 2. In situ study on SNU-9: (a) Adsorption of CO_2 at 195 K, (b) X-ray diffraction patterns measured during adsorption, and (c) X-ray diffraction patterns measured during desorption. Colors of adsorption points correspond to the latter of X-ray diffraction patterns.

106.98(11)°) in as made phase to strongly distorted square-pyramidal in narrow pore phase (adjacent angles range 58.92(10)—127.09(9)°). In opposite, the strongly distorted coordination geometry of Zn2 atom remained mostly unchanged upon the structural transition. Thus, in SNU-9_activated (or narrow pore form of the compound) only one carboxylic group O6—C16—O7 bridges Zn atoms in μ-carboxylato-κO:κO′ mode. The second one, O1—C1—O2 changes its coordination mode to chelate, coordinating by both oxygen atoms to Zn2. The O1 oxygen atom from the latter is also coordinated to Zn1 atom having a bridging function. Remaining two carboxylate groups O9—C30—O10 and O4—C15—O5 coordinate to Zn1 and Zn2 atoms in a bidentate mode with different Zn−O bond lengths [2.257(2), 2.045(2), 2.295(4) and 2.058(3) Å] (Figure 1).

Interestingly, the Zn···Zn distance in the SBU as well as distance between the nearest symmetry equivalent Zn atoms belonging to different frameworks in the evacuated structure are 3.192(6) and 7.385(1) Å, respectively, that is very close to the corresponding values in the open structure (3.210(8) Å and 7.629(4) Å). Thus, the flexibility of SNU-9 is not caused by mutual moving of the interpenetrated frameworks. Structures of activated and as made phases are stabilized by weak $\pi\cdots\pi$ interactions with the similar Cg···Cg distances (3.876(1) Å for activated and 3.909(1) Å for as made forms) between two phenyl rings that originate from two symmetrically independent $BPnDC^{2-}$ linkers, coordinating to the different Zn atoms in the chelate mode.

Looking on the ligands arrangement around the SBU in both phases along the same crystallographic direction, one can notice mostly the same orientation of 4,4′-bipyridines (depicted in blue in Figure 1) and one of BPnDC linkers (depicted in red in Figure 1). In contrast, the second BPnDC ligand (marked green in Figure 1) changes orientation in a such a way, that the opposing carboxylate group unfolds in the same direction with 4,4′-bipyridine.

A similar example of coordination changes in the paddle-wheel SBU during the "gate opening" was reported by Kitagawa et al. for $Zn_2(bdc)_2L$ (L = 2,3-difluoro-1,4-bis(4-pyridyl)-benzene) compound.[31] This compound is composed of "classical" Zn paddle-wheel unit, where the coordination geometry of Zn changes from square pyramidal to tetrahedral with simultaneous increasing of Zn···Zn distance from 3.00 Å in as made structure to 3.43 Å in the evacuated form.

The single net of SNU-9_ as-made crystal structure has square channels along [101] direction with 16.4 Å in diameter.

dx.doi.org/10.1021/ic4024844 | Inorg. Chem. 2014, 53, 1513−1520

After removal of guest molecules from the pores, the pores contract along b direction to 10.7 Å (Figure 1).

To estimate the porosity of as-made and evacuated phase of SNU-9, the geometric surface area was calculated using Poreblazer 3.0 program.[44] Using the nitrogen molecule as a probe, the specific geometric surface area was calculated as 1034 $m^2 g^{-1}$ for "large pore" and 10.5 $m^2 g^{-1}$ for "narrow pore" form of SNU-9.

In Situ Adsorption via Powder X-ray Diffraction Study. To track the structural changes time-resolved, in situ powder X-ray diffraction investigation of SNU-9_activated was performed using CO_2 (195 K) and N_2 (77 K) as adsorptive.

The X-ray powder diffraction pattern, measured on evacuated sample at 195 K, involves only reflections, corresponding to the "narrow pore" phase (Figure S3 Supporting Information). This pattern was used for Pawley refinement (see Figure S1 Supporting Information). As expected, the refined unit cell parameters as well as unit cell volume from the data collected at 195 K are smaller in comparison to the latter obtained from the single crystal X-ray diffraction experiment performed at room temperature (Table S1 Supporting Information).

The adsorption branch of the carbon dioxide physisorption isotherm shows two distinct steps which is indicative for some structural changes (Figure 2a). The material starts to adsorb the gas at low relative pressures, showing "type I" behavior in the relative pressure region $0.001 \leq p/p_0 \leq 0.15$. The gas uptake amount to 40 $cm^3 g^{-1}$ and is in a good agreement with the accessible void of 12.8% estimated from the crystal structure of the "narrow pore" phase (Table 2). Pore volumes, calculated from the CO_2 adsorption isotherm and from the crystal structure of as-made phase amount to 0.39 $cm^3 g^{-1}$ and 0.38 $cm^3 g^{-1}$, respectively, showing a strong correlation between structural and adsorption data.

Table 2. Porosity Relevant Data for SNU-9

	SNU-9 evacuated	SNU-9 as made
unit cell volume (Å^3)	7334(2)	10182(3)
solvent accessible void (% of unit cell)	12.8	40.8
geometrical surface area ($m^2 g^{-1}$)	10.5	1034

X-ray diffraction patterns, collected in the relative pressure range $0.001 \leq p/p_0 \leq 0.15$ show significant changes in the peak intensity, as well as appearance of some new peaks (Figure 2b) indicating the formation of an intermediate phase (Supporting Information Figure S8). Unfortunately all attempts to index the patterns of intermediate phase were without success, probably because of presence of reflections from different phases.

Further pressure increase leads to the second step in the adsorption isotherm. At the relative pressure of 0.3 the isotherm reaches a second plateau with saturation uptake of nearly 190 $cm^3 g^{-1}$ (Figure 2a), accompanied with the phase transition to the CO_2@SNU-9 structure.

It should be mentioned that even at $p/p_0 = 0.97$, the (200) reflex from the "narrow pore" could be seen as a shoulder of main peak in the pattern of CO_2@SNU-9 (Figure S4, Supporting Information). Obviously, some of the crystallites (probably some large crystals) are not subjected to the transformation process and stay in the narrow pore form. The accurate comparison of the diffractograms for CO_2@SNU-9 and SNU-9_as-made reveals, that the gas loaded compound is not identical with the solvent containing phase (Figure S5 Supporting Information).

Indexing of the CO_2@SNU-9 powder XRD pattern collected at $p/p_0 = 0.974$ results in a monoclinic cell ($C2/c$ space group) with cell parameters quite similar to this of as made phase (Table 3). The a and c lattice constants are slightly shorter and monoclinic β angle decreases from 104.1° to 99.1°. Since b lattice parameter increases, the unit cell with nearly the same volume results. The size of the channels along [101] direction of a single net increases from 10.7 Å (evacuated phase) to 17.2 Å (CO_2@SNU-9) along b direction (Figure 3).

The desorption branch of the isotherm shows "type I" run in the whole pressure region. Up to p/p_0 0.1 the XRD pattern comprises only peaks indicative for open state of the framework (Figure 2c). At relative pressure close to 0.1, XRD patterns indicate the formation of the transition state, similar to that observed at the same relative pressure during the adsorption. Interestingly, based on the powder XRD data, the intermediate phase is presented during the desorption in very narrow pressure range (much narrower than during the adsorption).

The X-ray powder diffraction patterns, measured in the region $1 \times 10^{-3} \leq p/p_0 \leq 4 \times 10^{-2}$ show the smooth transition from the transition state to the empty structure, whereas the powder pattern of evacuated compound after CO_2 adsorption again shows some peaks of CO_2@SNU-9, indicating, that the part of the sample does not transform to the "narrow pore" form (Supporting Information Figure S6). Obviously, the material has some kind of "memory effect" hindering the complete reorganization. Even evacuation and heating up to 333 K does not transform the compound to the initial evacuated state.

The in situ physisorption of nitrogen at 77 K was performed on the sample used for CO_2 adsorption and additionally evacuated in vacuum at 333 K for 1 h.

The adsorption branch of the isotherm shows a different shape in comparison to that measured on a fresh activated sample (the adsorption is shifted to the higher relative pressure) (Figure 4b). In contrast to CO_2 adsorption, the nitrogen adsorption isotherm shows only one distinct step. The material starts to adsorb nitrogen at $p/p_0 = 0.05$, showing no changes in the powder XRD in the lower pressure region (Figure 4a). The intermediate phase is also formed, but at $p/p_0 = 0.04$, the XRD pattern already contains also the reflexes of

Table 3. Unit Cell Parameters of All Investigated Phases from Pawley Refinement

	a (Å)	b (Å)	c (Å)	β (deg)	V (Å^3)
evacuated SNU-9 (195 K)	26.2908(6)	10.5265(3)	27.0871(1)	104.661(2)	7252(3)
CO_2@SNU-9(195 K)	20.5112(3)	19.5795(3)	25.7508(4)	99.156(1)	10210(1)
N_2@SNU-9(77 K)	21.1230(3)	18.8229(3)	26.4228(4)	104.108(1)	10188(1)
as-made SNU-9 (293 K)[a]	21.150(4)	18.850(4)	26.200(5)	102.90(3)	10182(3)

[a]Cell parameters are obtained from single crystal X-ray diffraction data.

dx.doi.org/10.1021/ic4024844 | Inorg. Chem. 2014, 53, 1513−1520

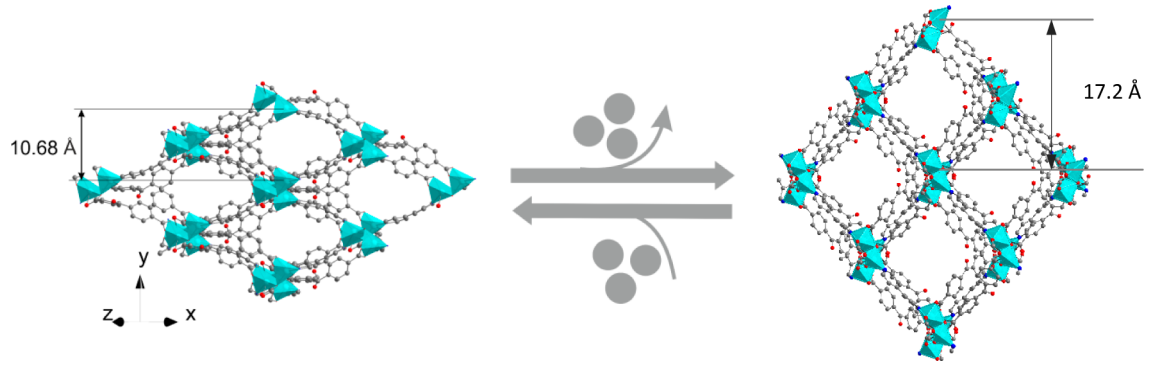

Figure 3. View on a single framework of SNU-9 along [101] direction before (left) and after CO_2 adsorption (right).

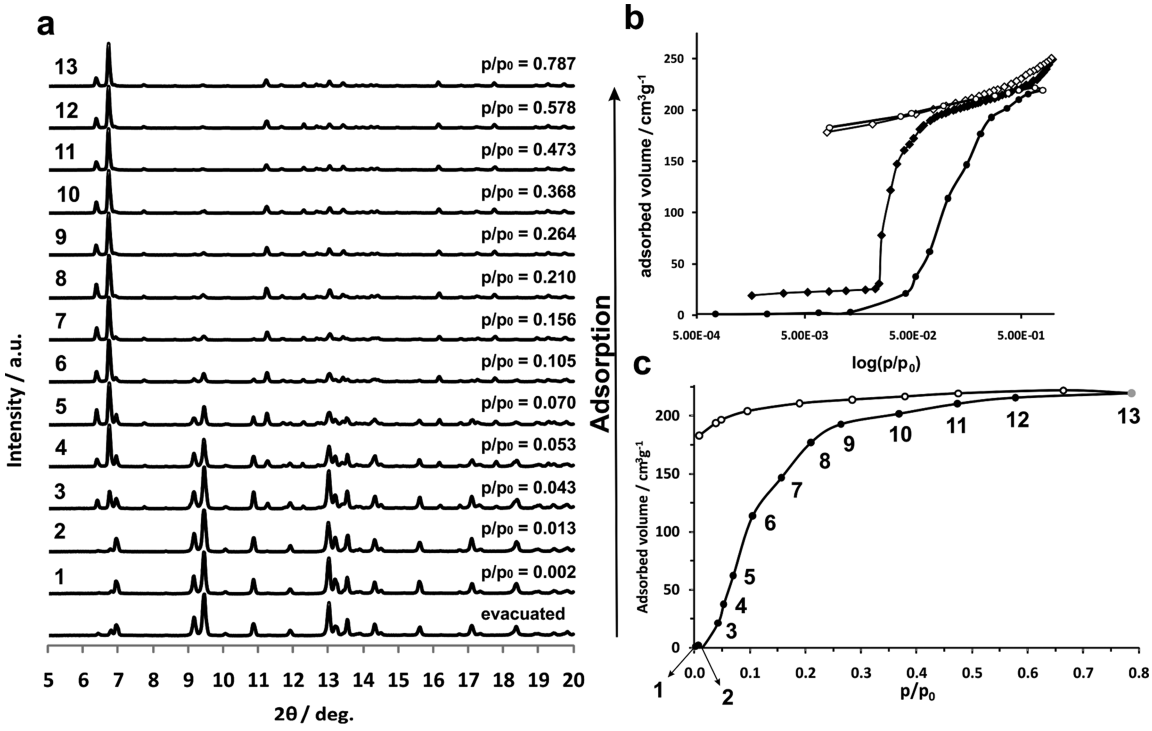

Figure 4. In situ study on SNU-9: (a) X-ray diffraction patterns, measured during adsorption; (b) semilogarithmic plot of adsorption isotherms measured on fresh activated sample (spheres) and the sample after CO_2 adsorption (squares); and (c) N_2 adsorption isotherm, measured in situ at 77 K. Colors of adsorption points correspond to the latter of X-ray diffraction patterns.

N_2@SNU-9 open phase and could not be recorded as phase pure. Obviously, the existence range for intermediate phase is very narrow in this case.

The adsorption isotherm reaches a plateau at $p/p_0 = 0.6$ with saturation uptake of 220 $cm^3\ g^{-1}$. This value is somewhat lower, in comparison to the reported earlier (262 $cm^3\ g^{-1}$) (Figure 4c).[34]

The nitrogen filled sample contains also as an impurity the "narrow pore" phase, but in significantly lower quantity in comparison to the CO_2 filled sample (Supporting Information Figure S7). Furthermore, the peaks remaining from CO_2@SNU-9 in the XRD pattern of the starting material disappear, and the final powder diffraction pattern of N_2@SNU-9 is equal to the powder pattern of SNU-9_as-made compound (Figure 5). The powder pattern recorded at $p/p_0 = 0.8$ was successfully used for the Pawley refinement (Supporting Information Figure S2). The cell parameters of N_2@SNU-9 agree very well with the cell parameters of SNU-9_as-made (Supporting Information Table S2).

The desorption isotherm was measured down to $p/p_0 = 8.5 \times 10^{-3}$. In this pressure region no changes in XRD patterns could be observed, thus the "open structure" does not transform even at low pressures (Supporting Information Figure S9).

CONCLUSIONS

The intrinsic structural dynamics during adsorption/desorption of guest molecules on SNU-9 were analyzed by powder X-ray diffraction and simultaneous adsorption experiments. The crystal structures of as made and solvent free phases were solved from single crystal X-ray diffraction data. During the activation, Zn−O bond rearrangement occurs, giving rise to a change in coordination environment of Zn atoms of activated compound. Such rearrangement leads to the contraction of the structure in *b* direction accompanied by decrease in the unit cell volume and accessible void volume. The adsorption of CO_2 at 195 K and N_2 at 77 K proceeds in a different way: the formation of intermediate phase during the CO_2 adsorption

dx.doi.org/10.1021/ic4024844 | Inorg. Chem. 2014, 53, 1513−1520

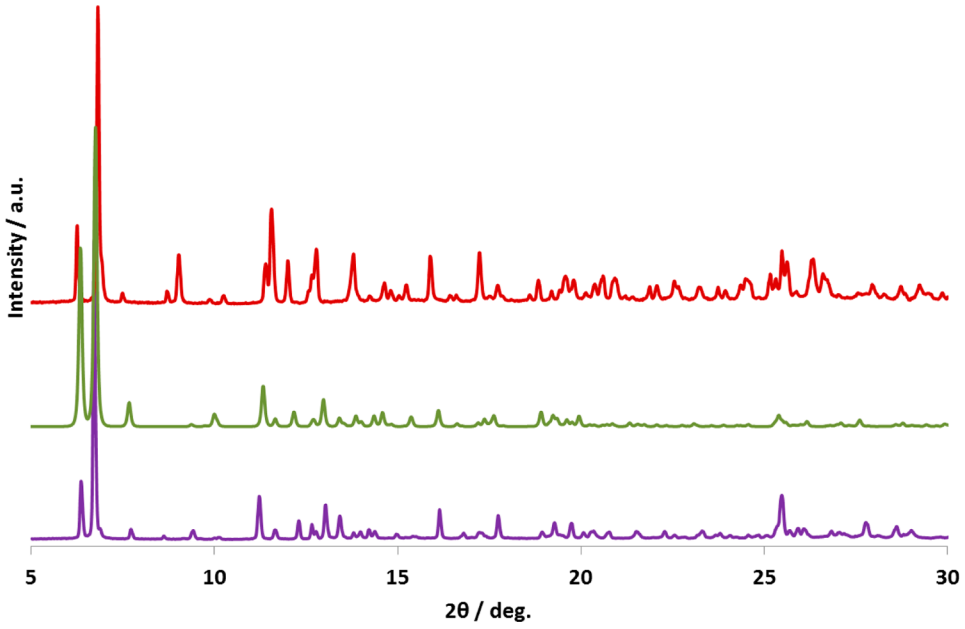

Figure 5. Comparison of calculated XRD pattern for SNU-9_as-made with XRD pattern of SNU-9 filled with N_2 at 77 K (p/p_0 = 0.8), and XRD pattern of SNU-9 filled with CO_2 at 195 K (p/p_0 = 0.98).

could be postulated, while the transformation from narrow pore form to the open structure occurs quasi in one step by nitrogen physisorption. The gas loaded compounds have also different final crystal structures at relative pressure around p/p_0 = 0.9. According to the powder diffraction data, the structure of N_2@SNU-9 is identical to the structure of as made compound, the cell volume of CO_2@SNU-9 is slightly higher.

■ ASSOCIATED CONTENT

Supporting Information

Pawley refinement plots, structural data, and powder X-ray diffraction patterns. This material is available free of charge via the Internet at http://pubs.acs.org.

■ AUTHOR INFORMATION

Corresponding Author

*E-mail: Stefan.Kaskel@chemie.tu-dresden.de. Fax: +49-351-463-37287.

Notes

The authors declare no competing financial interest.

■ ACKNOWLEDGMENTS

This work was supported by Federal Ministry of Education and Research (BMBF Project No 05K10OD3) and Helmhotz Zentrum Berlin für Materialien und Energie.

■ REFERENCES

(1) Yaghi, O. M.; Li, H. L.; Davis, C.; Richardson, D.; Groy, T. L. *Acc. Chem. Res.* **1998**, *31*, 474−484.
(2) Eddaoudi, M.; Moler, D. B.; Li, H. L.; Chen, B. L.; Reineke, T. M.; O'Keeffe, M.; Yaghi, O. M. *Acc. Chem. Res.* **2001**, *34*, 319−330.
(3) Lin, W. B.; Rieter, W. J.; Taylor, K. M. L. *Angew. Chem., Int. Ed.* **2009**, *48*, 650−658.
(4) Ockwig, N. W.; Delgado-Friedrichs, O.; O'Keeffe, M.; Yaghi, O. M. *Acc. Chem. Res.* **2005**, *38*, 176−182.
(5) Furukawa, H.; Ko, N.; Go, Y. B.; Aratani, N.; Choi, S. B.; Choi, E.; Yazaydin, A. Ö.; Snurr, R. Q.; O'Keeffe, M.; Kim, J.; Yaghi, O. M. *Science* **2010**, *329*, 424−428.
(6) Farha, O. K.; Eryazici, I.; Jeong, N. C.; Hauser, B. G.; Wilmer, C. E.; Sarjeant, A. A.; Snurr, R. Q.; Nguyen, S. T.; Yazaydın, A. Ö.; Hupp, J. T. *J. Am. Chem. Soc.* **2012**, *134*, 15016−15021.
(7) Suh, M. P.; Park, H. J.; Prasad, T. K.; Lim, D.-W. *Chem. Rev.* **2011**, *112*, 782−835.
(8) Sumida, K.; Rogow, D. L.; Mason, J. A.; McDonald, T. M.; Bloch, E. D.; Herm, Z. R.; Bae, T.-H.; Long, J. R. *Chem. Rev.* **2011**, *112*, 724−781.
(9) Lin, X. A.; Champness, N. R.; Schröder, M. *Top. Curr. Chem.* **2010**, *293*, 35−76.
(10) Dueren, T.; Sarkisov, L.; Yaghi, O. M.; Snurr, R. Q. *Langmuir* **2004**, *20*, 2683−2689.
(11) Stoeck, U.; Krause, S.; Bon, V.; Senkovska, I.; Kaskel, S. *Chem. Commun.* **2012**, *48*, 10841−10843.
(12) Yan, Y.; Yang, S.; Blake, A. J.; Lewis, W.; Poirier, E.; Barnett, S. A.; Champness, N. R.; Schroder, M. *Chem. Commun.* **2011**, *47*, 9995−9997.
(13) Padmanaban, M.; Muller, P.; Lieder, C.; Gedrich, K.; Grunker, R.; Bon, V.; Senkovska, I.; Baumgartner, S.; Opelt, S.; Paasch, S.; Brunner, E.; Glorius, F.; Klemm, E.; Kaskel, S. *Chem. Commun.* **2011**, *47*, 12089−12091.
(14) Builes, S.; Roussel, T.; Vega, L. F. *AIChE J.* **2011**, *57*, 962−974.
(15) Maes, M.; Alaerts, L.; Vermoortele, F.; Ameloot, R.; Couck, S.; Finsy, V.; Denayer, J. F. M.; De Vos, D. E. *J. Am. Chem. Soc.* **2010**, *132*, 2284−2292.
(16) Maes, M.; Vermoortele, F.; Alaerts, L.; Couck, S.; Kirschhock, C. E. A.; Denayer, J. F. M.; De Vos, D. E. *J. Am. Chem. Soc.* **2010**, *132*, 15277−15285.
(17) Li, Y.-S.; Liang, F.-Y.; Bux, H.; Feldhoff, A.; Yang, W.-S.; Caro, J. *Angew. Chem., Int. Ed.* **2010**, *49*, 548−551.
(18) Yoon, M.; Srirambalaji, R.; Kim, K. *Chem. Rev.* **2011**, *112*, 1196−1231.
(19) Corma, A.; Garcia, H.; Xamena, F. X. L. *Chem. Rev.* **2010**, *110*, 4606−4655.
(20) Xamena, F.; Abad, A.; Corma, A.; Garcia, H. *J. Catal.* **2007**, *250*, 294−298.
(21) Wu, C. D.; Lin, W. B. *Angew. Chem., Int. Ed.* **2007**, *46*, 1075−1078.
(22) Horike, S.; Shimomura, S.; Kitagawa, S. *Nat. Chem.* **2009**, *1*, 695−704.

(23) Kanoh, H.; Kondo, A.; Noguchi, H.; Kajiro, H.; Tohdoh, A.; Hattori, Y.; Xu, W.-C.; Inoue, M.; Sugiura, T.; Morita, K.; Tanaka, H.; Ohba, T.; Kaneko, K. *J. Colloid Interface Sci.* **2009**, *334*, 1−7.
(24) Millange, F.; Serre, C.; Ferey, G. *Chem. Commun.* **2002**, 822−823.
(25) Klein, N.; Hoffmann, H. C.; Cadiau, A.; Getzschmann, J.; Lohe, M. R.; Paasch, S.; Heydenreich, T.; Adil, K.; Senkovska, I.; Brunner, E.; Kaskel, S. *J. Mater. Chem.* **2012**, *22*, 10303−10312.
(26) Yanai, N.; Uemura, T.; Inoue, M.; Matsuda, R.; Fukushima, T.; Tsujimoto, M.; Isoda, S.; Kitagawa, S. *J. Am. Chem. Soc.* **2012**, *134*, 4501−4504.
(27) Serra-Crespo, P.; van der Veen, M. A.; Gobechiya, E.; Houthoofd, K.; Filinchuk, Y.; Kirschhock, C. E. A.; Martens, J. A.; Sels, B. F.; De Vos, D. E.; Kapteijn, F.; Gascon, J. *J. Am. Chem. Soc.* **2012**, *134*, 8314−8317.
(28) Chen, X. Y.; Vinh-Thang, H.; Rodrigue, D.; Kaliaguine, S. *Ind. Eng. Chem. Res.* **2012**, *51*, 6895−6906.
(29) Xiao, B.; Byrne, P. J.; Wheatley, P. S.; Wragg, D. S.; Zhao, X.; Fletcher, A. J.; Thomas, K. M.; Peters, L.; EvansJohn, S. O.; Warren, J. E.; Zhou, W.; Morris, R. E. *Nat. Chem.* **2009**, *1*, 289−294.
(30) Miller, S. R.; Wright, P. A.; Devic, T.; Serre, C.; Férey, G. r.; Llewellyn, P. L.; Denoyel, R.; Gaberova, L.; Filinchuk, Y. *Langmuir* **2009**, *25*, 3618−3626.
(31) Seo, J.; Bonneau, C.; Matsuda, R.; Takata, M.; Kitagawa, S. *J. Am. Chem. Soc.* **2011**, *133*, 9005−9013.
(32) Chen, S.-S.; Chen, M.; Takamizawa, S.; Wang, P.; Lv, G.-C.; Sun, W.-Y. *Chem. Commun.* **2011**, *47*, 4902−4904.
(33) Salles, F.; Maurin, G.; Serre, C.; Llewellyn, P. L.; Knöfel, C.; Choi, H. J.; Filinchuk, Y.; Oliviero, L.; Vimont, A.; Long, J. R.; Férey, G. *J. Am. Chem. Soc.* **2010**, *132*, 13782−13788.
(34) Park, H. J.; Suh, M. P. *Chem. Commun.* **2010**, *46*, 610−612.
(35) Bon, V.; Senkovska, I.; Wallacher, D.; Heerwig, A.; Klein, N.; Zizak, I.; Feyerherm, R.; Dudzik, E.; Kaskel, S. *Microporous Mesoporous Mater.* **2013**, DOI: 10.1016/j.micromeso.2013.12.024.
(36) *Material Studio 5.0*, Release 5.0; Accelrys Software, Inc.: San Diego, CA, 2009.
(37) Mueller, U.; Darowski, N.; Fuchs, M. R.; Forster, R.; Hellmig, M.; Paithankar, K. S.; Puhringer, S.; Steffien, M.; Zocher, G.; Weiss, M. S. *J. Synchrotron Rad.* **2012**, *19*, 442−449.
(38) Winn, M. D.; Ballard, C. C.; Cowtan, K. D.; Dodson, E. J.; Emsley, P.; Evans, P. R.; Keegan, R. M.; Krissinel, E. B.; Leslie, A. G. W.; McCoy, A.; McNicholas, S. J.; Murshudov, G. N.; Pannu, N. S.; Potterton, E. A.; Powell, H. R.; Read, R. J.; Vagin, A.; Wilson, K. S. *Acta. Crystallogr., Sect. D* **2011**, *67*, 235−242.
(39) Sheldrick, G. *Acta Crystallogr., Sect. A* **2008**, *64*, 112−122.
(40) Dybtsev, D. N.; Chun, H.; Kim, K. *Angew. Chem., Int. Ed.* **2004**, *43*, 5033−5036.
(41) Klein, N.; Herzog, C.; Sabo, M.; Senkovska, I.; Getzschmann, J.; Paasch, S.; Lohe, M. R.; Brunner, E.; Kaskel, S. *Phys. Chem. Chem. Phys.* **2010**, *12*, 11778−84.
(42) Aijaz, A.; Lama, P.; Bharadwaj, P. K. *Eur. J. Inorg. Chem.* **2010**, *2010*, 3829−3834.
(43) Spek, A. *Acta Crystallogr., Sect. D* **2009**, *65*, 148−155.
(44) Sarkisov, L.; Harrison, A. *Mol. Simul.* **2011**, *37*, 1248−1257.